

This work features collaboration between research groups at Max Planck Institute for Solid State Research (Germany), ALKALOID AD (Macedonia) and Faculty of Natural Sciences and Mathematics, SS. Cyril and Methodius University (Macedonia)

On the hydrates of codeine phosphate: the remarkable influence of hydrogen bonding on the crystal size

The sesquihydrate and hemihydrate of codeine phosphate differ by one water molecule per codeine cation. The influence of this molecule on the internal crystal structure and how it translates into the external crystal size and shape are reported.

### As featured in:



See Tomče Runčevski et al.,  
*Chem. Commun.*, 2014, **50**, 6970.

## On the hydrates of codeine phosphate: the remarkable influence of hydrogen bonding on the crystal size†

Cite this: *Chem. Commun.*, 2014, 50, 6970

Received 24th February 2014,  
Accepted 28th February 2014

DOI: 10.1039/c4cc01430h

[www.rsc.org/chemcomm](http://www.rsc.org/chemcomm)

**Codeine phosphate forms three hydrates and two anhydrides. The sesquihydrate and hemihydrate, which differ by one water molecule, are stable at room temperature. The influence of this molecule on the internal crystal structure and how it translates into the external crystal shape are reported.**

Codeine is a natural alkaloid, which is extracted from the opium poppy plant. It is a well-known narcotic, analgesic, antitussive and anti-diarrhoeal active pharmaceutical ingredient (API) and has a long history, for example, in the treatment of mild to moderate pain, coughs, diarrhoea, and irritable bowel syndrome.<sup>1</sup> It is such a widely used narcotic that it can be found in the WHO Model List of Essential Drugs. Codeine is frequently marketed in the form of its phosphate salt (**COP**, Chart 1), only two hydrates of which are commercially used in the preparation of pharmaceutical formulations: the sesquihydrate (**COP-S**; 1.5 water equivalents per codeine cation) and the hemihydrate (**COP-H**; 0.5 water equivalents). Recently, thermoanalytical studies (TGA/DSC) were published, revealing that, upon heating, **COP-S** transforms into an unstable monohydrate (**COP-M**), which subsequently converts into **COP-H**. Heating above 100 °C leads to the formation of two anhydrous forms (**COP-AI** and **COP-AII**).<sup>2</sup>

Even though **COP** is an important API, there are many unanswered questions regarding its solid state properties. Surprisingly, especially given the fact that it is an API that has been used in the pharmaceutical industry for more than half a century, the published crystallographic research is scarce. The only crystal structure detailed in the literature is that of **COP-H**.<sup>3</sup> Among the most

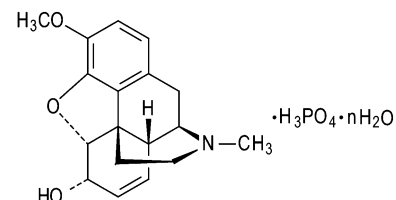


Chart 1 Structural formula of the codeine phosphate *n*-hydrate.

significant reasons for such poor crystallographic knowledge of **COP** is its crystallization behaviour; it yields single crystals of **COP-H**, but a polycrystalline bulk of **COP-S** (Fig. 1). It is known that changes in the crystal structure alter the physical properties of a solid, including the crystallization behaviour.<sup>4</sup> The effect of composition on the crystallization behaviour displayed here is rather impressive as is governed by the one water molecule difference between **COP-S** and **COP-H**. The ability of the water molecule to change the crystal structure (*e.g.* *via* hydrogen bonding networks) is recognised,<sup>4</sup>

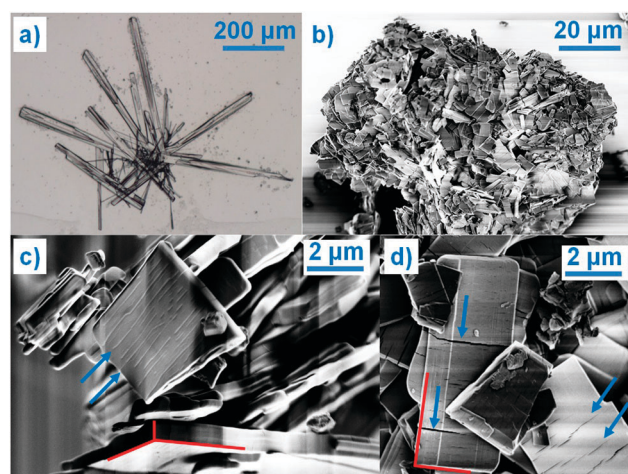


Fig. 1 (a) Optical microscopy image of **COP-H** single crystals, and (b–d) SEM images of **COP-S** polycrystalline particles (the red lines are a guide to the eye for the microcrystals habit whereas the blue arrows indicate the cracks perpendicular to the largest crystal axis).

<sup>a</sup> Max Planck Institute for Solid State Research, Heisenbergstrasse 1, 70569 Stuttgart, Germany. E-mail: t.runclevski@flf.mpg.de

<sup>b</sup> Research & Development, ALKALOID AD, Aleksandar Makedonski 12, 1000 Skopje, Macedonia

<sup>c</sup> Institute of Chemistry, Faculty of Natural Sciences and Mathematics, SS. Cyril and Methodius University, Arhimedova 5, 1000 Skopje, Macedonia

† Electronic supplementary information (ESI) available: Description of sample preparation, Crystallographic details and the Rietveld plot of **COP-S**. CCDC 988910, FTIR spectra. For ESI and crystallographic data in CIF or other electronic format see DOI: 10.1039/c4cc01430h



and the **COP** hydrates stand out as extreme examples of how it translates into the physical size and shape of the crystal. Moreover, when dealing with APIs, the physics of the solid is very important, as it might affect a number of properties, including (but not limited to) toxicity, bioavailability, chemical stability or shelf life.<sup>5</sup> Therefore, an understanding of the role of one additional water molecule in how the **COP** crystal grows is highly desirable.

In the course of the present research, as well as during previous studies on the solid state transformations and solvatomorphism,<sup>2</sup> recrystallization of **COP** in different solvents always leads to single crystals of **COP-H** and powder samples of **COP-S**. Given the polycrystalline nature of **COP-S**, here, its crystal structure was solved using X-ray powder diffraction (XRPD), which is an emerging technique for structure solutions of pharmaceuticals.<sup>6</sup> Indexing was performed using first principles by the iterative use of singular value decomposition, followed by Pawley fitting and the simulated annealing approach to solve the crystal structure, which was later refined by the Rietveld method, confirming the solution and, in addition, providing information on the microstructure.<sup>†‡</sup> The asymmetric unit of **COP-S** is composed of two codeine cations adopting the characteristic T conformation known from related compounds of the opiate family.<sup>3</sup> One slight difference in the crystal structures of the codeine cations in **COP-S** and **COP-H** is the orientation of the methoxy group. The crystal packing of the cations is similar to the one in **COP-H**, as shown in Fig. 2(a-d). The similar packing of the codeine cations cannot solely account for the difference in crystallization behaviour. Irrespective of being similarly packed, independent codeine units are linked differently to other constituents of the asymmetric unit. In **COP-H**, two cations are linked together through (codeine)-O-H···O-(codeine) hydrogen bonds, employing the hydroxy and methoxy groups, the hydroxy group is

additionally bonded to the water molecule and moreover, both codeine cations are bonded to the phosphate anions *via* (codeine)-N-H···O-(phosphate) hydrogen bonds (Fig. 2(e)).<sup>3</sup> The hydrogen bonding scheme of **COP-S** differs significantly from that of **COP-H**. In one of the codeine cations, the protonated amino group and the hydroxy group are both bonded to water molecules, whereas in the other cation the same groups are bonded to the oxygen atoms of the phosphate anions (Fig. 2(f)).

The crucial difference between the **COP-H** and **COP-S** structures is the hydrogen-bonding network of the phosphate anions and water molecules. The adjacent phosphate anions of **COP-H** are pairwise joined together by hydrogen bonds to build an extended ribbon chain on which the water molecules and codeine cations are attached (Fig. 2(g)). The presence of an additional water molecule leads to the completely different hydrogen bonding scheme in **COP-S**, where a complex 2D layer is formed (Fig. 2(h)).<sup>§</sup> The phosphate anions are joined pairwise, additionally linking to water molecules as well as the hydroxy and protonated amino groups of the codeine cations. Three crystallographically different water molecules are present, two of them bonded to the codeine cations and one only participating in the formation of the phosphate–water 2D layer. The differences in the hydrogen bonding motifs are clearly reflected in the IR spectra.<sup>†</sup> As previously observed,<sup>2</sup> the spectrum of **COP-H** exhibits two sharp peaks ( $3503$  and  $3460\text{ cm}^{-1}$ ) and two shoulders ( $3540$  and  $3401\text{ cm}^{-1}$ ) ascribed to mixed N-H and O-H vibrations. The extensive hydrogen bonding observed in the structure of **COP-S** helped to explain the large redshift, manifested by the appearance of a broad band with superimposed shoulders ( $\sim 3270$ ,  $3457$  and  $3500\text{ cm}^{-1}$ ).

The disparity in the crystal structures of **COP-H** and **COP-S** can be related to the differences in their crystallization behaviour and crystal shape. As previously indicated,<sup>3</sup> a systematic comparison of the phosphate ribbon chain motif in **COP-H** with related structures points out that this very simple synthon is favoured by the packing of dihydrogen phosphate anions. Thus, the propagation of the chain and attached codeine cations from the surrounding solution forms druses of single crystals with the prismatic habit. With careful evaporation of the solvent, crystals of **COP-H** larger than  $500\text{ }\mu\text{m}$  in length can be easily grown (Fig. 1(a)). In contrast, **COP-S** crystallizes as extensively cracked prismatic crystals rarely exceeding a few micrometres in size (Fig. 1(b-d)). Rietveld refinements indicated that average domain sizes range within  $0.1$  and  $0.15\text{ }\mu\text{m}.$ <sup>‡</sup> It is known that the crystal growth is heavily affected by the presence of defects in the structure, which often cause growth termination. The introduction of such defects in the simple phosphate chains in **COP-H** is less likely as compared to the complicated 2D network in **COP-S**, where the absence and/or displacement of, for example, a single  $\text{H}_2\text{O}$  molecule, can severely disrupt the 2D structure. Interestingly, this 2D layer is packed perpendicularly to the largest unit cell axis (Fig. 2(b and d)), which possibly correlates to the cracks in the microcrystals, perpendicular to the longest crystal axis (Fig. 1(c and d)).

The well-defined, 2D hydrogen-bonded phosphate–water network, on which the codeine cations are attached, ensures the

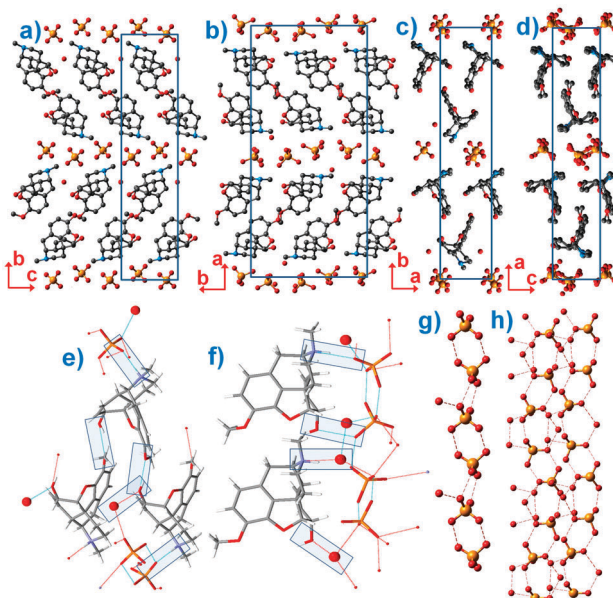


Fig. 2 Crystal packing of **COP-H** shown in (a) and (c) and **COP-S** in (b) and (d). Hydrogen bonding of the codeine cations of (e) **COP-H** and (f) **COP-S**. The extended hydrogen bonding network of phosphate anions and water molecules of (g) **COP-H** and (h) **COP-S**. The unit cell content of **COP-H** is doubled for better comparison with **COP-S**.



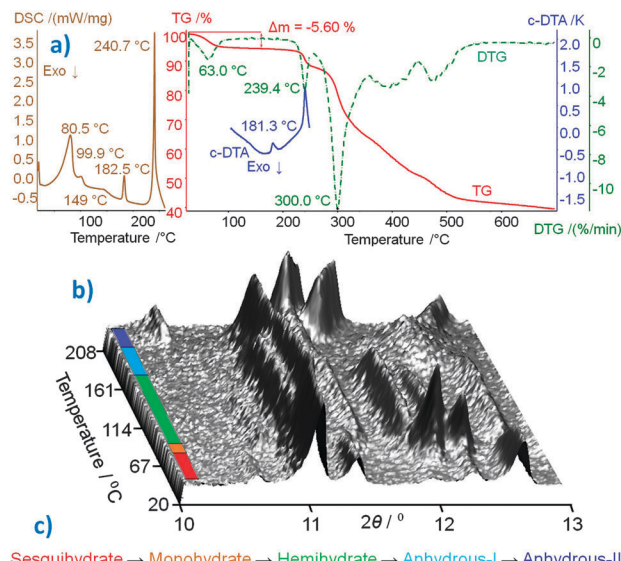


Fig. 3 (a) Thermoanalytical characterization curves of **COP-S**.<sup>2</sup> (b) 3D projection of scattered X-ray intensity of **COP-S** presented as a function of the diffraction angle and temperature, the different phases are colour coded according to the (c) dehydration/polymorphism sequence.

very stable crystal packing of **COP-S**, which is stable at room temperature (RT) and under both ambient and saturated humidity conditions.<sup>2a</sup> **COP-S** was proved to be the highest hydrate, with 1.5 water molecules per codeine cation. The study of its thermally-induced process was revisited, complementing the published thermoanalytical data (summarized in Fig. 3(a))<sup>2</sup> with *in situ* crystallographic analysis. The aim of this was to detect the unstable **COP-M** form and to firmly establish the dehydration scheme of this pharmaceutically important compound. The DSC curve (Fig. 3(a)) indicated that four endothermic transitions before thermal decomposition occurred (starting at  $\sim 240$  °C, as shown by the TG and DTG curves). The second peak visible on the DSC curve (at 99.9 °C) was not detected in the DTG or *c*-DTA analyses. To confirm that this low-energy effect is not due to the experimental error or an artefact, temperature-resolved XRPD data were collected *in situ* (Fig. 3(b)).<sup>¶</sup> The changes in the scattered X-ray intensity of **COP-S** as a function of the diffraction angle and temperature nicely complement the DSC results, showing four transitions below 210 °C. The first three thermal effects are assigned to the dehydration sequence: **COP-S**  $\rightarrow$  **COP-M**  $\rightarrow$  **COP-H**  $\rightarrow$  **COP-AI**, followed by one polymorphic transition, **COP-AI**  $\rightarrow$  **COP-AII**, before total degradation takes place (Fig. 3c). An interesting observation is that, upon heating, unlike all other forms, **COP-AII** exhibits a large and continuous diffraction peak shift towards higher angles, indicating significant unit cell positive thermal expansion.

In summary, **COP** crystallizes as two hydrates at RT, sesquihydrate **COP-S** (1.5 H<sub>2</sub>O) and hemihydrate **COP-H** (0.5 H<sub>2</sub>O), whereas the intermediate **COP-M** form (1 H<sub>2</sub>O) is unstable. At high temperatures, two anhydrous polymorphs are produced (**COP-AI** and **COP-AII**). The presence of 1.5 H<sub>2</sub>O molecules per codeine cation leads to a stable form at RT and at ambient and

saturated humidities. Losing 0.5 H<sub>2</sub>O molecules per codeine cation equivalent results in instability (**COP-M**) and a further loss of 0.5 H<sub>2</sub>O molecules once again stabilizes the structure (**COP-H**). **COP-S** and **COP-H** have similarly packed codeine cations and differ only by one water molecule per cation. However, this single water molecule makes a huge difference in the hydrogen bonding network. This detail of the internal crystal structure highly influences the external crystal shape and stability. **COP-H** forms single crystals, whereas **COP-S** crystallizes as cracked microcrystals with domains as small as 0.1 μm.

The efforts of Mr Wied, Mrs Kuševska, Mrs Popovic and Dr Nuss in making the international transport of the drug possible are very much appreciated. Mrs Knöller is acknowledged for recording the SEM images and Mr Beardsworth for proof-reading the manuscript. TR thanks the IMPRS-CMS. The authors thank the anonymous reviewers for the valuable comments and suggestions which significantly improve the quality of this communication.

## Notes and references

‡ Crystallographic details of **COP-S**:  $2\theta$  range 3–66°, X-ray radiation with  $\lambda = 1.540596$  Å, data collection time of 24 h. Space group  $P2_12_12_1$ , unit cell:  $a = 33.4761(7)$  Å,  $b = 16.0612(3)$  Å,  $c = 7.1921(2)$  Å;  $R_{\text{Bragg}} = 0.0225$ ,  $R_{\text{exp}} = 0.0099$ ,  $R_{\text{wp}} = 0.0348$ ,  $R_{\text{p}} = 0.0285$ , 89 refined parameters.

§ For measuring the hydrogen bonding, the intermolecular O–O distances were studied and the values are deposited in the CIF file.

¶ *In situ* XRPD patterns were collected at each degree upon heating, in a  $2\theta$  range of 10–13°,  $\lambda = 1.540596$  Å, with a data collection time of 2 min.

- (a) A. J. Atkinson, H. F. Adler and A. C. Ivy, *J. Am. Med. Assoc.*, 1943, **121**, 646; (b) N. B. Eddy, H. Friebel, K.-J. Hahn and H. Halbach, *Bull. W. H. O.*, 1968, **38**, 673; (c) N. B. Eddy, H. Friebel, K.-J. Hahn and H. Halbach, *Bull. W. H. O.*, 1969, **40**, 425.
- (a) G. Petruševski, S. Ugarković and P. Makreski, *J. Mol. Struct.*, 2011, **993**, 328; (b) G. Petruševski, M. Kajdžanoska, S. Ugarković, I. Micovski, G. Bogoeva-Gaceva, G. Jovanovski and P. Makreski, *Vib. Spectrosc.*, 2012, **63**, 60.
- C. Langes, T. Gelbrich, U. J. Griesser and V. Kahlenberg, *Acta Crystallogr., Sect. C: Cryst. Struct. Commun.*, 2009, **65**, 419.
- (a) J. Bernstein, *Polymorphism in Molecular Crystals*, Oxford University Press, Oxford, 2002; (b) G. R. Desiraju, *Angew. Chem., Int. Ed. Engl.*, 1995, **34**, 2311; (c) M. Wenger and J. Bernstein, *Cryst. Growth Des.*, 2008, **8**, 1595; (d) C. Näther, I. Jess, P. G. Jones, C. Taouss and N. Teschmit, *Cryst. Growth Des.*, 2013, **13**, 1676; (e) D. Braga, F. Grepioni and L. Maini, *Chem. Commun.*, 2010, **46**, 6232; (f) C. Janiak, *Dalton Trans.*, 2003, 2781; (g) C. B. Aakeroy, M. E. Fasulo and J. Desper, *Mol. Pharmaceutics*, 2007, **4**, 317; (h) B. Rodriguez-Spong, C. P. Price, A. Jayasankar, A. J. Matzger and N. Rodriguez-Hornedo, *Adv. Drug Delivery Rev.*, 2004, **56**, 241; (i) M. R. Caira, *Mol. Pharmaceutics*, 2007, **4**, 310; (j) A. Othman, J. S. O. Evans, I. Radosavljević Evans, R. K. Harris and P. Hodgkinson, *J. Pharm. Sci.*, 2007, **96**, 1380.
- (a) S. R. Byrn, R. R. Pfeiffer and J. G. Stowell, *Solid State Chemistry of Drugs*, SSCI Inc., West Lafayette, IN, 2nd edn, 1999; (b) S. L. Morissette, O. Almarsson, M. L. Peterson, J. F. Remenar, M. J. Read, A. V. Lemmo, S. Ellis, M. J. Cima and C. R. Gardner, *Adv. Drug Delivery Rev.*, 2004, **56**, 275; (c) N. Shan and M. J. Zaworotko, *Drug Discovery Today*, 2008, **13**, 440; (d) J. Chen, B. Sarma, J. M. B. Evans and A. S. Myerson, *Cryst. Growth Des.*, 2011, **11**, 887; (e) O. Almarsson and M. J. Zaworotko, *Chem. Commun.*, 2004, 1889.
- (a) R. E. Dinnebier, P. Sieger, H. Nar, K. Shankland and W. I. F. David, *J. Pharm. Sci.*, 2000, **89**, 1465; (b) K. Sugimoto, R. E. Dinnebier and M. Zakrzewski, *J. Pharm. Sci.*, 2007, **96**, 3316; (c) L. Vella-Zarb, R. E. Dinnebier and U. Baisch, *Cryst. Growth Des.*, 2013, **13**, 4402; (d) K. D. M. Harris and E. Y. Cheung, *Chem. Soc. Rev.*, 2004, **33**, 526.